DETECTION OF β-LACTAM ANTIBIOTICS BASED ON CONJUGATED ANTIBODY WITH GOLD NANORODS BY LOCALIZED SURFACE PLASMON RESONANCE SPECTROMETER**

M. Aghamirzaei [1,2*], M. S. Khiabani [1], H. Hamishehkar [3], R. R. Mokarram [1], M. Amjadi [1]

[1] University of Tabriz, Tabriz, Iran, e-mail: aghamirzaei.ma88@gmail.com
[2] Food and Drug Administration, Alborz University of Medical Sciences, Karaj, Iran
[3] Drug Applied Research Center at Tabriz University of Medical Sciences, Tabriz, Iran

This study aimed to determine the β-lactam antibiotics (ampicillin, amoxicillin, penicillin G, oxacillin, and carbenicillin) using conjugated antibody along with gold nanorods (AuNRs). For this purpose, XRD, ATR-FTIR spectroscopy, transmission electron microscopy, and dynamic light scattering were utilized to detect the crystallinity, to identify functional groups involved in the synthesis of AuNRs, and to measure the size of the AuNRs, respectively. In this regard, pH of 9 and a concentration of 9.6 μg of antibody at 1 mL poly (4-styrenesulfonic acid (PSS))-modified AuNRs solution were selected as the best levels of pH and concentration of antibody for the conjugation of antibody with PSS-modified AuNRs. Thereafter, the maximum wavelength rates of the PSS-modified AuNRs, conjugation of antibody with PSS-modified AuNRs, and detection of antibiotics (from 1 nM to 1 mM) with PSS-modified AuNRs-PAb were recorded using a micro-volume spectrophotometer system. The results indicate that the LSPR absorption wavelength of PSS-modified AuNRs is red-shifted by increasing the concentration of β-lactam antibiotics. By increasing the concentrations of ampicillin, penicillin G, and carbenicillin, the maximum wavelength changed, and after the saturation of the antibiotic concentration, the curve reached a plateau. Correspondingly, this indicated that the antibody had a similar behavior in the detection of these antibiotics. However, regarding amoxicillin, the saturation concentration is much higher, which indicate that the antibody is more specific for its detection. In contrast, for oxacillin, saturation occurred immediately, demonstrating that the antibody had an extremely low detection capability for this antibiotic. Finally, the findings showed that the antibody was sensitive to 1 nM of five studied β-lactam antibiotics.

Keywords: *localized surface plasmon resonance spectrometer, β-lactam antibiotics, polyclonal antibody of β-lactam, gold nanorods, poly(4-styrenesulfonic acid) solution, cetyltrimethylammonium bromide, conjugation.*

ОБНАРУЖЕНИЕ β-ЛАКТАМНЫХ АНТИБИОТИКОВ НА ОСНОВЕ КОНЪЮГИРОВАННЫХ АНТИТЕЛ С НАНОСТЕРЖНЯМИ ЗОЛОТА С ПОМОЩЬЮ СПЕКТРОМЕТРА ЛОКАЛИЗОВАННОГО ПОВЕРХНОСТНОГО ПЛАЗМОННОГО РЕЗОНАНСА

M. Aghamirzaei [1,2*], M. S. Khiabani [1], H. Hamishehkar [3], R. R. Mokarram [1], M. Amjadi [1]

УДК 543.42;620.3

[1] Тебризский университет, Тебриз, Иран, e-mail: aghamirzaei.ma88@gmail.com
[2] Университет медицинских наук Альборз, Фардис, Альборз, Карадж, Иран
[3] Центр прикладных исследований лекарственных средств при Тебризском университете медицинских наук, Тебриз, Иран

(Поступила 10 марта 2021)

Для определения β-лактамных антибиотиков (ампициллина, амоксициллина, пенициллина G, оксациллина и карбенициллина) использованы конъюгированные антитела с наностержнями золота (AuNR). Методы XRD, ATR-FTIR-спектроскопии, TEM и DLS применялись для обнаружения кри-

**Full text is published in JAS V. 89, No. 1 (http://springer.com/journal/10812) and in electronic version of ZhPS V. 89, No. 1 (http://www.elibrary.ru/title_about.asp?id=7318; sales@elibrary.ru).

сталличности, идентификации функциональных групп, участвующих в синтезе AuNR, и для измерения размера AuNR соответственно. Значения pH 9 и концентрации 9.6 мкг антител 1 мл раствора поли(4-стиролсульфоновой кислоты (PSS), модифицированного AuNR, выбраны как лучшие значения pH и концентрации антител для конъюгации с AuNR, модифицированными PSS. Максимумы λ_{max} AuNR, модифицированных PSS, конъюгации антител с AuNR, модифицированных PSS, и обнаружения антибиотиков (от 1 нМ до 1 мМ) с AuNR-PAb, модифицированными PSS, зарегистрированы с помощью микрообъемного спектрофотометра. Результаты показывают, что длина волны поглощения локализованного поверхностного плазмонного резонанса для AuNR, модифицированных PSS, смещена в красную область из-за увеличения концентрации β-лактамных антибиотиков. С увеличением концентрации ампициллина, пенициллина G и карбенициллина положение максимума изменяется и после насыщения антибиотиком кривая выходит на плато, т. е. антитело имеет аналогичное поведение при обнаружении этих антибиотиков. Для амоксициллина концентрация насыщения намного выше, т. е. антитело более специфично для его обнаружения. В случае оксациллина насыщение происходит быстро, демонстрируя чрезвычайно низкую способность антител к обнаружению этого антибиотика. Показано, что антитела чувствительны к концентрации 1 нМ пяти изученных β-лактамных антибиотиков.

Ключевые слова: *спектрометр локализованного поверхностного плазмонного резонанса, β-лактамные антибиотики, поликлональные антитела β-лактама, наностержни золота, раствор поли(4-стиролсульфоновой кислоты), бромид цетилтриметиламмония, конъюгация.*

Introduction. Antibiotics of the β-lactam group are included in a wide variety of antimicrobial agents used for the treatment of bacterial infections of animals in livestock farming. β-Lactams consists of the following four groups: penicillins, cephalosporins, carbapenems, and monobactams. Residual β-lactams can seriously cause allergic reactions in food and also develop resistant strains in consumers. Moreover, these can lead to serious economic problems for milk and dairy product producers. For example, by decreasing the acid and flavor of butter and reducing the curdling of the milk, they can cause unsuitable ripening of cheese.

Antibiotics are mostly detected using an instrumental technique such as high-performance liquid chromatography/mass spectrometry (HPLC/MS) [1] and gas chromatography/mass spectrometry (GC/MS) [2]. In addition, sensors can be used based on an antibody-antigen interaction such as the enzyme-linked immunosorbent assay (ELISA) [3], fluorescence polarization immunoassay [4], immunosensor assay [5], and UV and localized surface plasmon resonance (LSPR) [6–8]. In this study, AuNRs were used. They synthesized chemically, whereas biosynthesized gold nanoparticles (AuNPs) from Chinese lettuce (CL) leave extract (*Brassica rapa var. pekinensis*) were used in [8]. There is no difference in the considered antibiotics classes in [8]. In this current study, the AuNRs were used (as a novelty), which has two transversal and longitudinal peaks while spherical nanoparticles have one peak of maximum wavelength. Therefore, the possibility of fast and fine detection would be higher in AuNRs. The detection limit considering the use of AuNRs as a spectrophotometry method was 1ng/mL, while the detection unit for ELISA [3] and fluorescence polarization immunoassay (in water and milk) [4] methods were 2 and 10 ng/mL and 20 μg/kg, respectively.

In recent years, AuNRs have been used to detect pharmaceutical samples due to their excellent properties such as unique optical and electronic properties, biocompatibility, stability, and high extinction coefficients [7, 9–19]. Additionally, AuNRs can be conjugated with the antibody and then used to detect antibiotics in terms of the colorimetric method (absorbance intensity change or change in the LSPR wavelength) [20]. Of note, the LSPR band is also produced in AuNRs due to collective oscillations of free electrons, which have a natural frequency of oscillation .When this frequency matches the frequency of incident radiation, a major LSPR band is produced with the property of light absorption. It was shown that there is a direct correlation between sensitivity of antibodies and changes in intensity of absorption and the maximum wavelength. If the antibody has high sensitivity, as the concentration of antibiotics increases, both the absorption intensity and the LSPR wavelength significantly change. But if the antibody has low sensitivity, the intensity wavelength does not change significantly. However, to apply this method, the antibody must be properly conjugated with the AuNRs. Therefore, several factors such as the amount of antibody and pH must be evaluated for proper conjugation [21]. This study aimed to use antibody conjugated with gold nanoparticles, in order to detect β-lactam antibiotics using the LSPR technique.

Materials. Sheep Polyclonal β-lactam antibody (PAb) was purchased from MyBioSource Co. (California, USA). Chloroauric acid ($HAuCl_4 \cdot 3H_2O$) was obtained from Jieding Tech Co. (Shanghai, China). More-

over, the ampicillin sodium salt, penicillin G potassium salt, amoxicillin, oxacillin sodium salt monohydrate, poly(4-styrenesulfonic acid) solution (PSS), cetyltrimethylammonium bromide (CTAB), silver nitrate ($AgNO_3$), sodium borohydride ($NaBH_4$), L-ascorbic acid (AA), and carbenicillin disodium salt were purchased from Sigma-Aldrich (St. Louis, USA). pH indicator paper and potassium carbonate were obtained from Merck (Darmstadt, Germany). Phosphate-buffered saline (PBS) powder was purchased from Biosera (France), and the other used chemicals were of analytical grade. Distilled water was purified using an ultrapure water system from Millipore (Bedford, MA, USA).

Methods. At this stage, Gold nanorods (AuNRs) were prepared in terms of the seed mediated growth procedure. The Au seeds were then synthesized by chemical reduction of $HAuCl_4$ with $NaBH_4$. The procedure was performed as follows: 7.5 mL CTAB (0.2 mM) was mixed with 250 μL $HAuCl_4$ (1 mM) and the mixture stirred magnetically. Next, 600 μL ice-cold $NaBH_4$ (10 mM) was added to this mixture. The solution's yellow color immediately turned to brown, indicating the formation of Au seeds. Subsequently, the Au seeds were used within 2–5 h. Notably, the growth solution for the formation of the AuNRs consisted of 4.7 mL CTAB (0.2 mM), 200 μL $HAuCl_4$ (1 mM), 40 μL $AgNO_3$ (4 mM), and 32 μL L-ascorbic acid (AA) (78.8 mM). Afterwards, 21 μL seed solution was added to the previous growth solution in order to initiate the growth of the AuNRs. After 12 h, the reaction was stopped, and the obtained AuNRs were purified by centrifuging the solution at 12,000 rpm for 5 min twice. Finally, the precipitates were collected and re-dispersed in deionized water [22].

The average size and charge of the AuNRs were both measured by dynamic light scattering using a particle size/zeta potential analyzer (Zetasizer Nano ZS, Malvern Instruments Ltd., UK).

To detect the morphology of the AuNRs, transmission electron microscopy (Jeol, Tokyo, Japan, at an accelerating voltage of 80,000 V and a magnification of 3,300,000) was used. Thereafter, AuNRs was ultrasonicated for 20 min and coated on the ultraclean carbon copper grid for analysis [17].

It is noteworthy that AuNRs are positively charged due to their CTAB, and antibodies are positively charged above the isoelectric pH, so no binding is possible in this regard. For this purpose, poly(4-styrenesulfonic acid) (PSS) was used to replace CTAB and then to establish antibody binding. The as-prepared CTAB-capped AuNRs are easily aggregated in non-aqueous solvent. In this step, surface modification was needed to enhance dispersion stability. As well, to investigate the relationship between LSPR peaks and the solution refractive index, PSS-modified AuNRs were employed. The preparation process of PSS-modified AuNRs was performed as follows: 12 mL of CTAB-capped AuNRs solution was centrifuged at 12,000 rpm for 10 min. Afterwards, this solution was dispersed in 12 mL of 2 mg/mL PSS solution aqueous solution (containing 6 mM NaCl) and magnetically stirred for 3 h. Finally, it was centrifuged at 12,000 rpm for 10 min, and the precipitate was re-dispersed either in water or in other solutions.

ATR-FTIR analysis was conducted for the identification of functional groups involved in the syntheses of both CTAB-capped AuNRs and PSS-modified AuNRs. The freeze-dried samples of CTAB-capped AuNRs and PSS-modified AuNRs were separately ground with KBR (FTIR grade) and then analyzed by an ATR-FTIR Nicolet Avatar 660 instrument (Nicolet, USA), using transmittance mode at 4 cm^{-1} resolution. At the end, the spectra were recorded ranged between 400 and 4000 cm^{-1} [23].

To detect the crystallinity of the CTAB-capped AuNRs and PSS-modified AuNRs, XRD (P Analytical, Philips PW 1830, The Netherlands) operating at 40 kV and 40 mA was applied, respectively. It is necessary to mention that the suspension containing AuNRs was dried for 24 h using a freeze dryer [24].

To determine the effect of pH on the conjugation of PAb with PSS-modified AuNRs, 500 μL of the PSS-modified AuNRs solution was put into an Eppendorf tube. Subsequently, pH of the PSS-modified AuNRs from 6 to 12 was adjusted by K_2CO_3. Next, 10 μg/mL of PAb was added into each tube, and the mixtures were gently stirred and allowed to react for 15 min at room temperature. Subsequently, 50 μL of 10% NaCl solution was added to each one of these tubes. Finally, the absorbance rate of each mixture was determined at 745 nm using a micro-volume spectrophotometer [25].

As well, different concentrations of PAb (0, 0.5, 1, 1.5, 2, 2.5, 3, 3.5, 4, 4.5, and 5 μg/mL) were added to 500 μL of the PSS-modified AuNRs solution with pH 9 to determine the effect of PAb concentration on the conjugation of PAb with PSS-modified AuNRs. Next, the obtained mixtures were gently stirred and then allowed to react for 20 min at room temperature. Finally, 50 μL of NaCl solution (10%) was added to each one of the tubes, and the absorbance rate of each mixture was measured at 745 nm [20].

To evaluate the detection accuracy of β-lactam antibiotics based on the conjugated PAb with PSS-modified AuNRs, different concentrations of β-lactam antibiotics (ampicillin, amoxicillin, penicillin G, oxacillin, and carbenicillin) ranging from 1 nM to 1 mM, were utilized. The detection criterion in this method

was considered in terms of the changes in the absorption intensity and the wavelength using a micro-volume spectrophotometer (Nano Mabna Iranian Co, Iran) within the wavelength range of 400 to 800 nm [26].

Results and discussion. *Dynamic light scattering (DLS) analysis.* Considering the dynamic light scattering results, the estimated average particle size distribution of AuNRs and average zeta potential value were determined as 51.5 nm (68.4%) and +15 mV, respectively (Figs. 1 and 2). The results of this study are consistent with the results of the study by Aljabali et al. [27]. Of note, DLS analysis of the generated AuNRs from leaf extract of *Ziziphus zizyphus* showed an average hydrodynamic diameter of 51.8 nm [27]. The zeta potential (electrokinetic potential) determines the nature and extent of the interaction between particles and liquid medium. Therefore, it is considered an important index of the colloidal stability of liquid dispersions. Moreover, this parameter may be positive or negative, but at values greater than -30 mV or +30 mV provide good quality and stability of nanoparticles, which can be stored for a long time. Accordingly, in this study, the zeta potential of AuNRs was estimated as +15 mV. The reason for the positive charge was the hydrophobic groups in the CTAB [28].

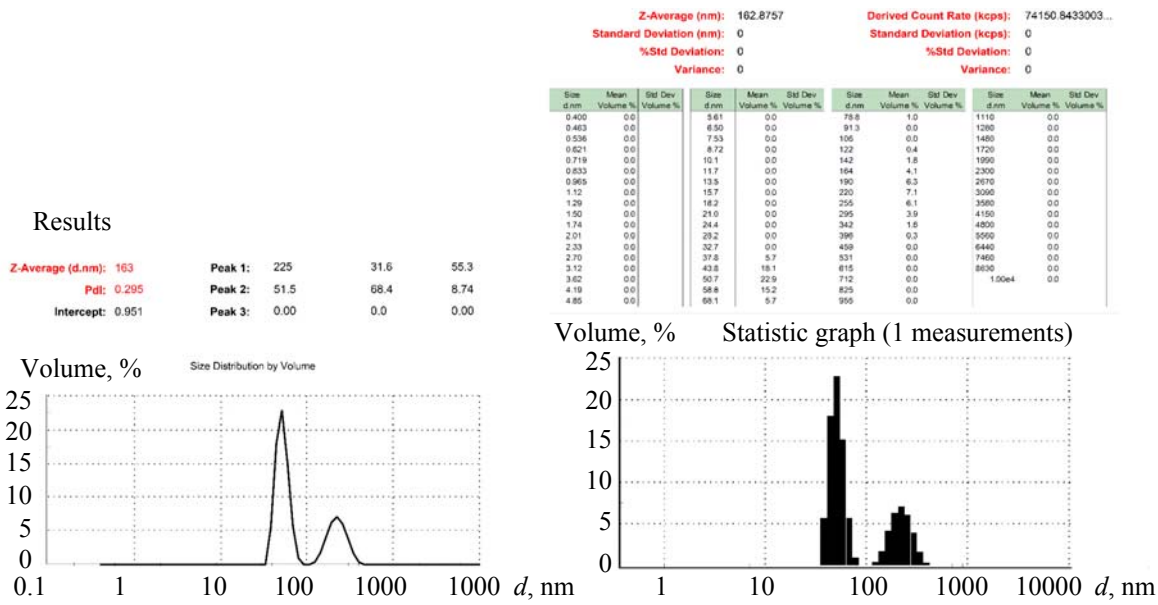

Fig. 1. DLS of gold nanorods (CTAB-capped AuNRs)

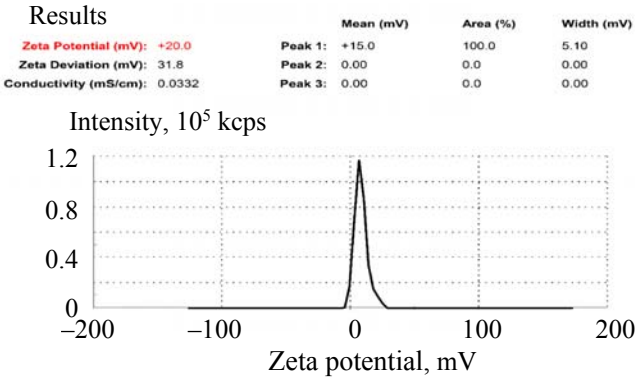

Fig. 2. Zeta potential of CTAB-capped AuNRs.

Figure 3 shows the images of the transmitted electron microscope (TEM) of the synthesized AuNRs in the current research. The images show that the obtained nanoparticles were rods with an aspect ratio of 3.6 (length of about 44 nm and diameter of about 12 nm). However, the significant differences in the size of the nanoparticles shown using the two techniques of DLS (51.5 nm) (Fig. 1) and TEM can be related to the adsorption of macromolecules and strongly hydrophilic compounds on the surface of the nanoparticles (in DLS technique). Correspondingly, this consequently resulted in high water sweating at the nanoparticles level and the radius of hydrodynamics to increase [29].

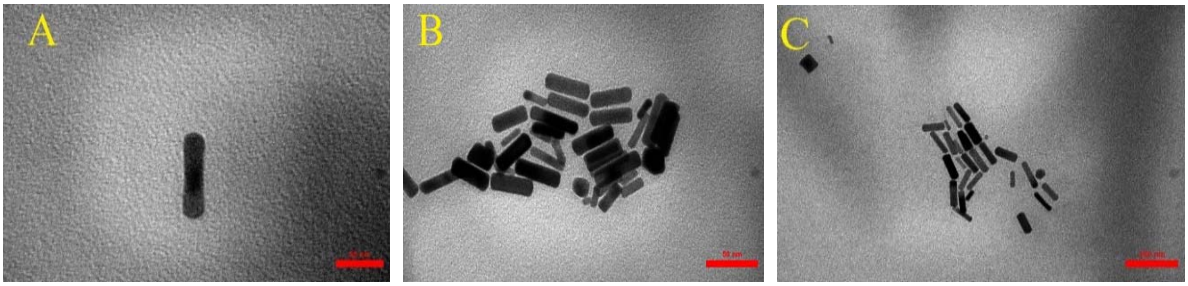

Fig. 3. TEM images of the CTAB-capped AuNRs.

Crystallographic patterns (XRD) of PSS replacement, instead of CTAB, are shown in Fig. 4. Structural analysis showed that the PSS-modified AuNRs had a crystalline structure with Miller indexes (111), (200), (220), (311), and (222) in the face-centered cubic structures (at 37.9, 44.2, 64.5, 77.5, and 81.5°, respectively). Similar results were also reported for AuNRs in the literature [30, 31]. By comparing the intensity of the peaks, it was cleared that the peak (111) was more intense than other peaks, as a result of which the crystalline nanoparticles were further formed in this direction compared to the other ones. The decrease in peak intensity may be due to the decrease in crystallinity resulting from the change in level. The reported peak values were also similar to the planes and face-centered cubic structures of AuNPs produced by the other green synthesis processes [32]. Usually, it can be said that the broadening of peaks in the XRD patterns of solids is associated with their particle size [33]. Notably, the XRD patterns match with the database of JCPDS file No. 00-004-0784.

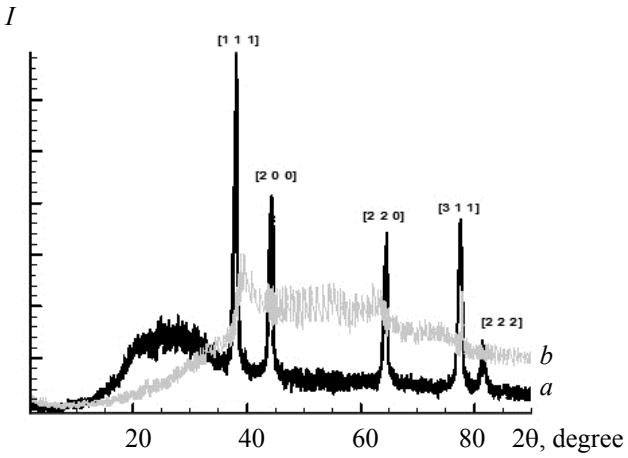

Fig. 4. X-ray diffraction spectrum of the CTAB-capped AuNRs (a) and PSS-modified AuNRs (b).

ATR-FTIR spectra of the CTAB-capped AuNRs and PSS-modified AuNRs are shown in Fig. 5. Accordingly, the CTAB-capped AuNRs showed peaks at ~2846.9 and ~2916.3 cm^{-1}, corresponding to CH_2. After the replacement of PSS in nanorods, peaks were created at 1176.5 and 1215.2 cm^{-1}, corresponding to the asymmetric O=S of the sulfonate group and also to the symmetric 1033.8 cm^{-1} O=S peak.

Effect of pH on conjugation of PAb with the PSS-modified AuNRs: pHs 6, 7, 8, 9, 10, 11, and 12, OD_{745} = 0.749±0.012[a], 0.722±0.013[b], 0.71±0.015[c], 0.702±0.005[d], 0.701±0.021[d], 0.69±0.061[d], and 0.703±0.006[d], respectively. (The obtained data are expressed as mean ± standard deviation (SD) of three independent experiments. Indexes (a, b, c, and d) show significant (p<0.05) differences between the means.) For this purpose, seven series of these solutions were made at different pHs at room temperature. As well, the absorbance rate of solutions was taken using a spectrophotometer at 745 nm. In this regard, the results indicated that by increasing pH, OD_{745} increases. The highest amount of OD_{745} was also observed at pH 9. Notably, no significant difference was observed in terms of OD_{745} between pH 9 and pH higher than 9. Therefore, pH 9 was selected as the best pH for the conjugation of antibody with the PSS-modified AuNRs. For a suitable conjugation, the pH of the medium should be greater than the isoelectric point of the antibody

[14]. At a pH lower than the antibody isoelectric pH, there is a negative charge for the protein, and conjugation cannot be thoroughly performed due to the negative charge of the nanoparticles as well as the repulsion between the nanoparticles and the antibodies. Nevertheless, at pHs higher than the isoelectric pH level, PSS-modified AuNRs can form a stable hydrophobic solution because of electrostatic interaction and van der Waals forces, which is called colloidal gold and is negatively charged [32, 34]. Thus, the positively charged antibodies and negatively charged colloidal gold solution conjugate firmly.

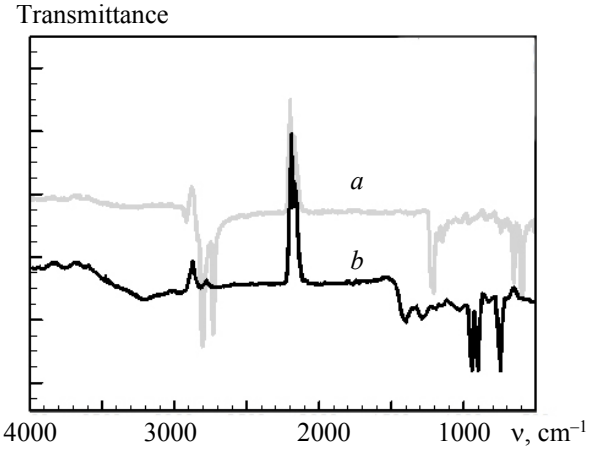

Fig. 5. ATR-FTIR spectrum of the CTAB-capped AuNRs (a) and PSS-modified AuNRs (b).

At the next stage, the effects of different concentrations of PAb (0.5, 1, 1.5, 2, 2.5, 3, 3.5, 4, 4.5, and 5) on the conjugation of PAb with the PSS-modified AuNRs were studied. Table 1 displays OD_{745} of the PSS-modified AuNRs, which were conjugated at different concentrations of AuNRs with pH of 9. The results indicated that OD_{745} decreases by increasing PAb concentration. As well, the smallest amount of OD_{745} was observed in 4.5 μg of PAb. No significant difference was observed in terms of OD_{745} between 4.5 μg PAb/500 μL and higher than 4.5 μg PAb /500 μL (Table 1). Therefore, 4.5 μg PAb /500 μL was selected as the best concentration of PAb for the conjugation of antibody with the PSS-modified AuNRs. In this regard, the results of some previous studies indicated that the optimal amount for a practical application can be adjusted to 120% of the PAb concentration minimum [25]. Therefore, a concentration of 4.8 μg of antibody at 500 μL of the PSS-modified AuNRs solution (i.e., 9.6 μg antibodies for 1 mL PSS-modified AuNRs) can be regarded as the best concentration for conjugation between the PSS-modified AuNRs and the antibody.

TABLE 1. Effect of PAb Concentration on Conjugation of PAb with the PSS-modified AuNRs

PAb concentration, μg	OD_{745}
0	0.989 ± 0.008^{a}
0.5	0.965 ± 0.006^{b}
1.0	0.959 ± 0.003^{bc}
1.5	0.955 ± 0.009^{bcd}
2.0	0.948 ± 0.012^{cde}
2.5	0.932 ± 0.015^{cde}
3.0	0.921 ± 0.007^{de}
3.5	0.918 ± 0.011^{de}
4.0	0.9 ± 0.003^{de}
4.5	0.98 ± 0.008^{de}
5.0	0.91 ± 0.006^{e}

N o t e. The obtained data are expressed as mean ± standard deviation (SD) of three independent experiments. Indexes (a, b, c, d, e) show significant (p<0.05) differences between the means.

The PAb-PSS-modified AuNRs were used for the detection of five β-lactam antibiotics (including ampicillin, penicillin G, amoxicillin, carbenicillin, and oxacillin). If the antibody has high sensitivity, as the

concentration of antibiotics increases, the intensity of absorption and the maximum wavelength would be exposed to more changes. However, if the antibody has low sensitivity, the intensity and wavelength do not change significantly. Figures 6 and 7 show the LSPR absorption spectra of the PSS-modified AuNRs-PAb solutions containing different concentrations of β-lactam antibiotics (including ampicillin, penicillin G, amoxicillin, carbenicillin, and oxacillin). Accordingly, the results indicated that when applying the concentrations of 0.01 μM of ampicillin, 0.1 μM of penicillin G, 1 μM of amoxicillin, 0.1 μM of carbenicillin, and 0.01 nM of oxacillin, the maximum wavelength (λ_{LSPR}) changed from 755 nm to 778, 736 to 785, 757 to 781, 753 to 770, and from 765 to 779 nm, respectively (Fig. 7). Therefore, this indicated that the antibiotics in these concentrations cause a redshift in wavelength due to the dipole coupling among the plasmon of the neighboring aggregated AuNRs.

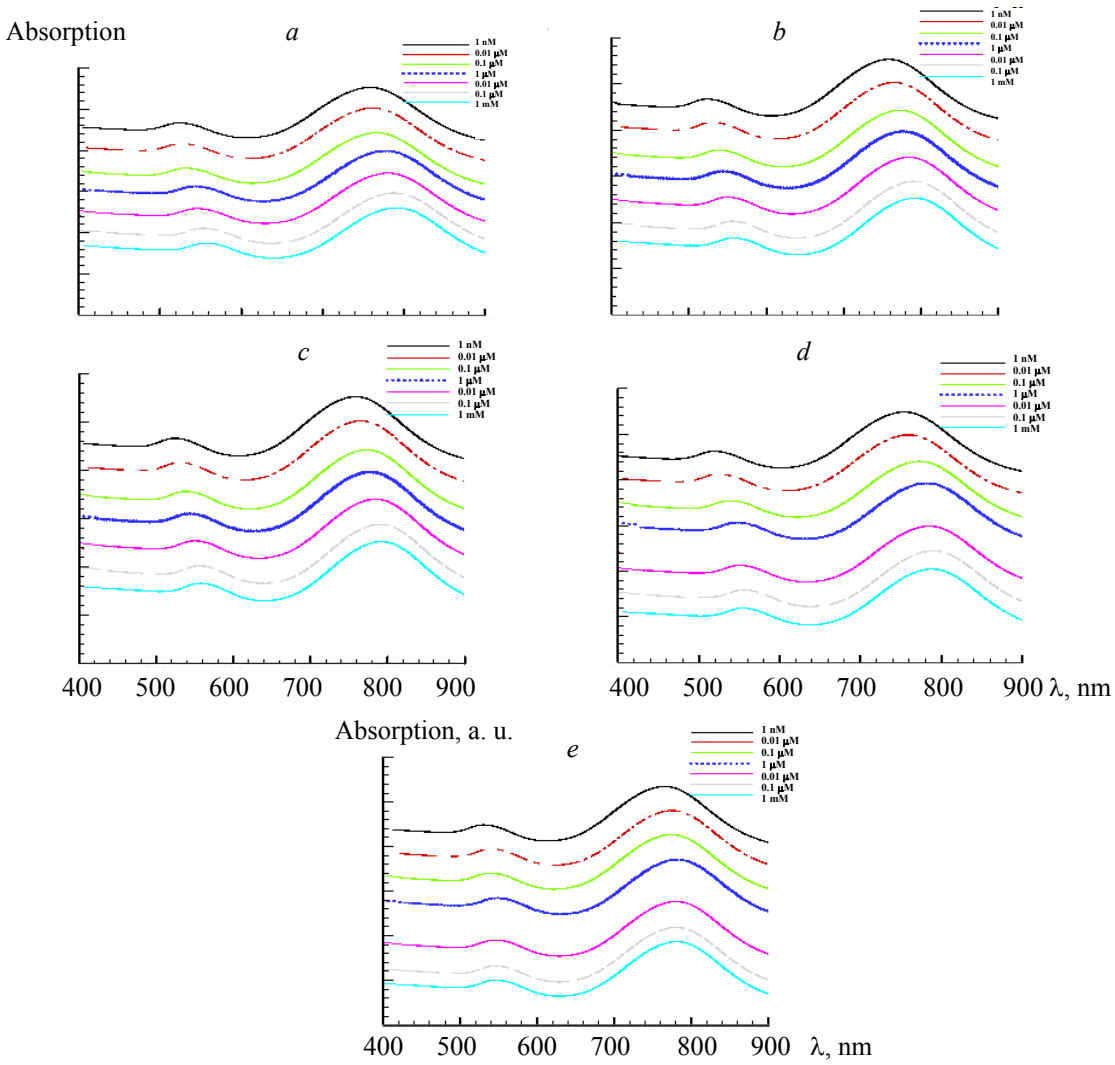

Fig. 6. (a) LSPR absorption spectra changes of the PSS-modified AuNRs solution after the addition of ampicillin concentration ranging from 1 nM to 1 mM, (b) after the addition of penicillin G concentration ranging from 1 nM to 1 mM, (c) after the addition of amoxicillin concentration ranging from 1 nM to 1 mM, (d) after the addition of carbenicillin concentration ranging from 1 nM to 1 mM, (e) after the addition of oxacillin concentration raning from 1 nM to 1 mM.

As a result, the intensity of absorption decreased and the peak shifted towards higher wavelengths. Furthermore, these results show that antibiotic binding to an antibody can increase the absorption of the maximum wavelength, demonstrating that the antibody is sensitive to 1 nM of β-lactam antibiotics (including ampicillin, penicillin G, amoxicillin, carbenicillin, and oxacillin). Because of the minimal amount of the

added antibiotics (1 nM), the intensity of absorption and the maximum wavelength have changed. Meanwhile, the results indicated that the maximum wavelength (λ_{LSPR}) increased along with increasing concentration of β-lactam antibiotics from 1 nM to 0.1 μM (ampicillin), 1 nM to 0.1 μM (penicillin G), 1 nM to 1 μM (amoxicillin), 1 nM to 0.01 μM (carbenicillin), and 1 nM to 1 μM (oxacillin), respectively. With excessive increase in antibiotics concentrations (0.1 mM to 1 mM ampicillin, 0.1 μM to 1 mM penicillin G, 0.01 μM to 1 mM amoxicillin, 0.01 μM to 1 mM carbenicillin, and 1 μM to 1 mM oxacillin), the maximum wavelength did not change, demonstrating the saturation state in the detection of antibiotics (Fig. 7). The reason may be that in high concentrations of the target molecule in the environment, the amount of accumulation would consequently increase. Moreover, in extremely high concentrations, it would become a vast aggregation. In other words, to increase the concentration of the antibiotic molecule in the environment, the amount of antibody bound to the target molecule should be increased. Consequently, the active site of antibody would be filled, and no empty capacity exists to detect antibiotic. Changes of wavelength peaks for ampicillin, penicillin G, and carbenicillin were similar. Accordingly, this indicates that the antibody has a similar behavior in the detection of these antibiotics. The maximum wavelength in the amoxicillin curve was compared to other β-lactam antibiotics at higher saturated concentrations. As a result, it can be concluded that this antibody has higher detectability, so it is more specific for the detection of amoxicillin. As shown in Fig. 7, oxacillin was saturated immediately and with a horizontal mode, indicating that the antibody has a very low detection capability for oxacillin. To explain more, the structure of the active site of the antibody was found to be more similar to the structure of amoxicillin, and on the other hand, the structure of the active site was less similar to the structure of oxacillin. Wang et al. [35] in their study showed that the maximum wavelength significantly migrates with increase in the concentration of kanamycin in the range of 10 nM to 1 μM.

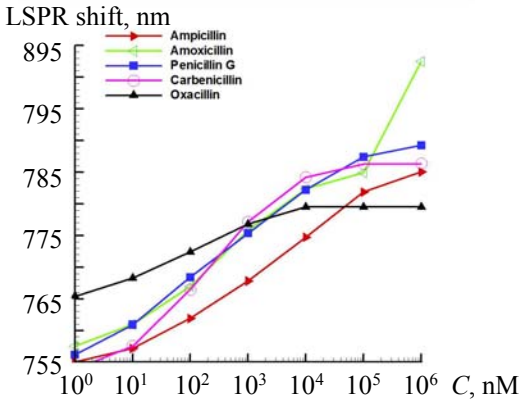

Fig. 7. LSPR shift absorption spectra changes of the PSS-modified AuNRs solution after the addition of β-lactam antibiotics (ampicillin, penicillin G, amoxicillin, carbenicillin, and oxacillin) concentration ranging from 1 nM to 1 Mm.

Conclusions. Gold nanorod-based colorimetric sensors have attracted much attention due to their excellent properties in the detection of residual drugs in food. In this study, the PSS-modified AuNRs conjugated with antibody were used for the colorimetric detection of β-Lactam antibiotics (including ampicillin, amoxicillin, penicillin G, oxacillin, and carbenicillin). Structural analysis performed by XRD showed that nanoparticles have a crystalline structure with Miller indexes (111), (200), (220), (311), and (222) in the face-centered cubic network. A pH of 9 and a concentration of 9.6 μg of antibody at 1 mL of the PSS-modified AuNRs solution were selected as the best pH and concentration of antibody for the conjugation. The LSPR wavelength of the PSS-modified AuNRs increased in higher concentration of β-lactam antibiotics. With increasing concentrations of ampicillin, penicillin G, and carbenicillin, the maximum wavelength changed, and after the saturation of antibiotics concentration the curve reached a plateau. However, regarding amoxicillin, the saturation concentration was much higher, indicating that the antibody is more specific for the detection of amoxicillin. In contrast, the system has a very low detection capability for this oxacillin. As well, the results show that the antibody is sensitive to 1 nM of five studied β-Lactam antibiotics.

Acknowledgments. This article is a part of a Ph.D. thesis approved at the University of Tabriz. This work was financially supported by Iran Nanotechnology Initiative Council (Grant code: 136472). The authors would like to thank Prof. Mohammad Javad Rasaee from Tarbiat Modares University; Dr. Seyed Mo-

hammad Amini from Iran University of Medical Sciences; and Mr. Gholamreza Behrouzi, Mr. Babak Farshid, Miss Zahra Abolghasemi-Fakhri, and Mrs. Samira Tizchang for their very useful comments. In addition, we thank Rojan Azma Company and its personnel for providing research equipment. Finally, we must thank Daneshmand Research & Development Institute and Mostazafan Foundation of Islamic Revolution.

REFERENCES

1. V. Tamošiūnas, A. Padarauskas, *Chromatographia*, **67**, 783–788 (2008), https://doi.org/10.1365/s10337-008-0579-5.
2. T. Śniegocki, A. Posyniak, J. Żmudzki, *Bull. Vet. Inst. Pulawy*., **51**, 59–64 (2007).
3. W. B. Shim, J. S. Kim, M. G. Kim, D. H. Chung, *J. Food Sci*., **78**, 1575–1581 (2013).
4. N. V. Gasilova, S. A. Eremin, *J. Anal. Chem*., **65**, 255–259 (2010), https://doi.org/10.1134/s1061934810030081.
5. F. Conzuelo, M. Gamella, S. Campuzano, D. G. Pinacho, A. J. Reviejo, M. P. Marco, J. M. Pingarrón, *Biosens. Bioelectron*., **36**, 81–88 (2012), https://doi.org/10.1016/j.bios.2012.03.044.
6. E. Kazemi, S. Dadfarnia, A. Mohammad, H. Shabani, M. R. Fattahi, J. Khodaveisi, *Spectrochim. Acta A: Mol. Biomol. Spectrosc*., **187**, 30–35 (2017), https://doi.org/10.1016/j.saa.2017.06.023.
7. N. Bi, M. Hu, H. Zhu, H. Qi, Y. Tian, H. Zhang, *Spectrochim. Acta A: Mol. Biomol. Spectrosc*., **107**, 24–30 (2013), https://doi.org/10.1016/j.saa.2013.01.014.
8. M. Aghamirzaei, M. Sowti Khiabani, H. Hamishehkar, R. Rezaei Mokaram, M. Amjadi, *J. Appl. Spectrosc.*, **88**, 174–184 (2021).
9. P. Cyganowski, D. Jermakowicz-bartkowiak, P. Jamroz, P. Pohl, A. Dzimitrowicz, *Coll. Surfase A*, **582**, 123886 (2019), https://doi.org/10.1016/j.colsurfa.2019.123886.
10. K. Hamaguchi, H. Kawasaki, R. Arakawa, *Coll. Surfase A: Physicochem. Eng. Aspects*, **367**, 167–173 (2010), https://doi.org/10.1016/j.colsurfa.2010.07.006.
11. Y. Huang, K. Ma, K. Kang, M. Zhao, Z. Zhang, Y. Liu, *Coll. Surfaces A: Physicochem. Eng. Aspects*, **421**, 101–108 (2013), https://doi.org/10.1016/j.colsurfa.2012.12.050.
12. X. Li, L. Jiang, Q. Zhan, J. Qian, S. He, *Colloids Surf. A: Physicochem. Eng. Aspects*, **332**, 172–179 (2009), https://doi.org/10.1016/j.colsurfa.2008.09.009.
13. S. Golmohammadi, M. Etemadi, *J. Appl. Spectrosc*., **86**, 925 (2019), https://doi.org/10.1007/s10812-019-00917-y.
14. C. Karami, A. Alizadeh, M. A. Taher, Z. Hamidi, B. Bahrami, *J. Appl. Spectrosc*., **83**, 687–693 (2016), https://doi.org/10.1007/s10812-016-0349-3.
15. G.P. Sahoo, H. Bar, D.K. Bhui, P. Sarkar, S. Samanta, S. Pyne, S. Ash, A. Misra, *Coll. Surfase A: Physicochem. Eng. Aspects*, **375**, 30–34 (2011), https://doi.org/10.1016/j.colsurfa.2010.11.033.
16. M. Singh, I. Sinha, A. K. Singh, R. K. Mandal, *Coll. Surfase A: Physicochem. Eng. Aspects*, **384**, 668–674 (2011), https://doi.org/10.1016/j.colsurfa.2011.05.037.
17. P. Vaccarello, L. Tran, J. Meinen, C. Kwon, Y. Abate, Y. Shon, *Coll. Surfase A: Physicochem. Eng. Aspects*, **402**, 146–151 (2012), https://doi.org/10.1016/j.colsurfa.2012.03.041.
18. Y. Yang, Q. Cui, Q. Cao, L. Li, *Coll. Surfase A: Physicochem. Eng. Aspects*, **503**, 28–33 (2016), https://doi.org/10.1016/j.colsurfa.2016.05.026.
19. J. Ye, K. Bonroy, F. Frederix, J. D. Haen, G. Maes, G. Borghs, *Coll. Surfase A: Physicochem. Eng. Aspects*, **321**, 313–317 (2008), https://doi.org/10.1016/j.colsurfa.2008.01.028.
20. K. S. McKeating, M. Couture, M. P. Dinel, S. Garneau-Tsodikova, J. F. Masson, *Analyst*, **141**, 5120–5126 (2016), https://doi.org/10.1039/c6an00540c.
21. L. Chen, Z. Wang, M. Ferreri, J. Su, B. Han, *J. Agric. Food Chem*., **57**, 4674–4679 (2009). https://doi.org/10.1021/jf900433d.
22. A. Singh, M. Sharma, A. Batra, *J. Optoelectron. Biomed. Mater*, **5**, 27–32 (2013).
23. C. George, I. Sergiel, A. Dzimitrowicz, P. Jamro, T. Kozlecki, P. Pohl, *Arab. J. Chem.*, **12**, No. 8 (2016), https://doi.org/10.1016/j.arabjc.2016.04.004.
24. J. Huang, Q. Li, D. Sun, Y. Lu, Y. Su, X. Yang, H. Wang, Y. Wang, W. Shao, N. He, J. Hong, C. Chen, *Nanotechnology*, **80**, 285–290 (2007), https://doi.org/10.1088/0957-4484/18/10/105104.
25. J. M. B. Res, G. Oza, S. Pandey, A. Gupta, R. Kesarkar, M. Sharon, W. Ambernath, *J. Microbiol. Biotechnol.*, **2**, 511–515 (2012).
26. C. Zhou, X. Zhang, X. Huang, X. Guo, Q. Cai, S. Zhu, *Sensors (Switzerland)*, **14**, 21872–21888 (2014),

https://doi.org/10.3390/s141121872.
27. A. Aljabali, Y. Akkam, M. Al Zoubi, K. Al-Batayneh, B. Al-Trad, O. Abo Alrob, A. Alkilany, M. Benamara, D. Evans, *Nanomaterials*, **8**, 1–15 (2018), https://doi.org/10.3390/nano8030174.
28. H. Mohammadi, M. Hafezi, S. Hesaraki, M. M. Sepantafar, *Nanomed. J.*, **2**, 217–222 (2015), https://doi.org/10.7508/nmj.
29. N. T. Ndeh, S. Maensiri, D. Maensiri, *Adv. Nat. Sci. Nanosci. Nanotechnol*., **8**, aa724a (2017), https://doi.org/10.1088/2043-6254/aa724a.
30. S. Goldmeier, K. De Angelis, K. R. Casali, C. Vilodre, F. Consolim-Colombo, A. B. Klein, R. Plentz, P. Spritzer, M. C. Irigoyen, *Am. J. Transl. Res*., **6**, 91–101 (2014), https://doi.org/10.1016/j.saa.2011.02.051.
31. S. A. Aromal, V. K. Vidhu, D. Philip, *Spectrochim. Acta A: Mol. Biomol. Spectrosc*., **85**, 99–104 (2012), https://doi.org/10.1016/j.saa.2011.09.035.
32. G. M. Corp, C. Astro, G. M. C. Safari, *Environ. Sci. Technol*., **37**, 3458–3466 (2003).
33. H. Borchert, E. V. Shevchenko, A. Robert, I. Mekis, A. Kornowski, G. Grübel, H. Weller, *Langmuir*, **21**, 1931–1936 (2005), https://doi.org/10.1021/la0477183.
34. H. Zhang, W. Li, Z. Sheng, H. Han, Q. He, *Analyst*, **135**, 1680–1685 (2010). https://doi.org/10.1039/c0an00025f.
35. X. Wang, Z. Mei, Y. Wang, L. Tang, *Talanta*, **136**, 1–8 (2017).